

# Switching-Ripple-Based Current Sharing for Paralleled Power Converters

David J. Perreault

Kenji Sato

John G. Kassakian

Massachusetts Institute of Technology  
Laboratory for Electromagnetic and Electronic Systems  
Cambridge, MA 02139 USA

**Abstract** - The paper presents the implementation and experimental evaluation of a new current-sharing technique for paralleled power converters. This technique uses information naturally encoded in the switching ripple to achieve current sharing, and requires no inter-cell connections for communicating this information. Practical implementation of the approach is addressed, and an experimental evaluation of the approach based on a 3-cell prototype system is also presented. It is shown that accurate and stable load sharing is obtainable over a wide load range with this approach.

## I. INTRODUCTION

Power conversion systems are sometimes constructed by paralleling many quasi-autonomous power converter cells (Fig. 1). Advantages of such a parallel, or *cellular*, converter architecture include high performance and reliability, modularity, and the ability to attain large system ratings [1,2].

One important characteristic of a parallel converter architecture is that the converter cells share the load current equally and stably. Good current-sharing behavior is important for reducing system losses and stresses, for improving system reliability, and for achieving desirable control characteristics. Current sharing is often implemented by interconnecting the cells via a communication bus over which information is shared [3-10]. While this approach is simple and effective, it is undesirable in many applications for reliability reasons, due to the need for additional interconnections among cells. Current sharing is sometimes obtained without additional

interconnections using droop methods, in which the voltage drops across the cell output impedances are used to enforce a degree of current sharing [11-13]. Unfortunately, by their nature, droop methods suffer from high output voltage regulation, which is unacceptable in many applications.

The proposed paper presents a current-sharing method which requires no additional interconnections among cells and which does not rely on output droop characteristics. This method, which was proposed but not validated in [14], uses information naturally encoded in the output switching ripple to achieve current-sharing among converter cells. The use of switching ripple to encode current-sharing information leads to performance advantages over other frequency-based approaches such as the output perturbation method of current sharing explored in [14,15]. Section II of the paper describes the operation of the new current-sharing method. Section III details one approach for implementing this method, and presents the design of a low-power prototype system which implements the approach. An experimental evaluation of the current-sharing method using the prototype system is presented in section IV. The final section of the paper presents conclusions and recommendations for further development of the current-sharing approach.

## II. THE SWITCHING RIPPLE METHOD

This paper considers the switching ripple method of current-sharing control proposed in [14] and illustrated in Fig. 2. In this approach, each converter cell is controlled such that its average output current is directly related to its switching frequency. As a result, the frequency content of the aggregate output ripple voltage contains information about the individual cell output currents. Each cell measures the output ripple voltage, and uses the information it contains to achieve current balance with the other cells.

Implementing a relationship between cell output current and switching frequency is typically straightforward, as many conversion approaches yield a natural relationship between them. For example, controlling a buck converter to operate at the edge of discontinuous conduction results in an inverse relationship between switching frequency and average output current (Fig. 3). Conversion approaches which do not exhibit a relationship between output current and switching frequency can often be modified to do so. For example, such a relationship could be achieved in a fixed-frequency PWM converter by adjusting the clock frequency (and PWM ramp slope) as a function of output current.

There are many methods by which the information in the aggregate output ripple voltage can be extracted and used to

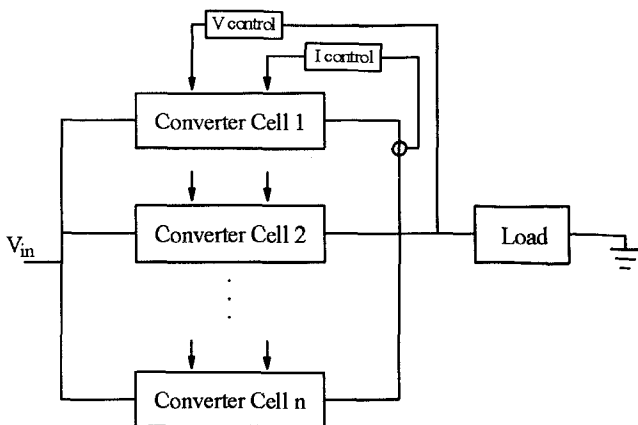


**Figure 1** A cellular converter architecture supplying a single load.

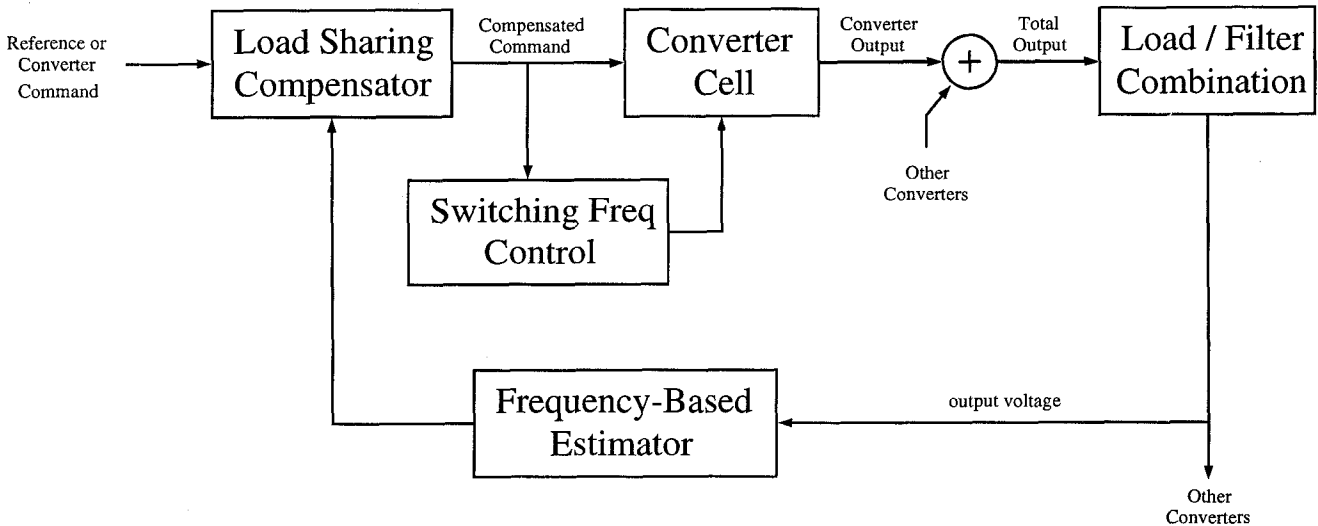


Figure 2 Schematic representation of the switching ripple method of current-sharing control.

achieve current sharing. In the approach considered here, each cell employs a frequency estimator which generates a positive (differential) signal when any other cell is operating at a lower switching frequency. Each cell uses this information to adjust its output such that no other cell is operating at a lower switching frequency. The cells thus converge to operating at the same switching frequency, and achieve current balance as a result. This approach is simple and robust, and is insensitive to the switching ripple harmonic content and waveform shape.

### III. PROTOTYPE SYSTEM IMPLEMENTATION

The current-sharing approach is demonstrated using a low-power 3-cell prototype system composed of buck converter cells operating at the edge of discontinuous conduction. Each cell has an inner current control loop, a middle voltage control loop, and an outer current-sharing control loop. The inner current control loop maintains operation of the cell at the edge of discontinuous conduction and inherently enforces a relationship between cell switching frequency and average output current. Current-sharing control is achieved in the prototype system by having each cell adjust its local reference voltage (used by the voltage control loop) if any other cell is operating at a lower switching frequency. Methods and circuits will be described for controlling cell switching patterns, making estimates of switching ripple frequency content based on output voltage measurements, and controlling the output voltage and

current balance among cells. A more detailed discussion of the design and implementation of the system can be found in [16,17].

#### A. Prototype System Power Stage

The prototype system uses low-power buck converter cells operating at the edge of discontinuous conduction under peak current control. Each cell has an inner current control loop which causes the cell output current to ramp between zero and twice the reference current  $i_{ref}$ , with an average value of  $i_{ref}$ . Each cell is designed to handle a peak current of 20 mA, yielding a per-cell load range of 1 - 10 mA. The system has a total output capacitance,  $C_f$ , of 45  $\mu$ F, and is resistively loaded.

Operation at the edge of discontinuous conduction yields an average output current (equal to one half of the peak output current) that is inversely proportional to the switching frequency. Specifically, for an approximately constant output voltage  $v_{cf}$ , we find

$$f_{sw} = \frac{v_{cf}(V_{in} - v_{cf})}{2V_{in}Li_{ref}} \quad (1)$$

For example, in the prototype system, with  $L = 125$  mH,  $V_{in} = 10$  V, and  $v_{cf} = 5$  V, full load for a cell corresponds to a 1

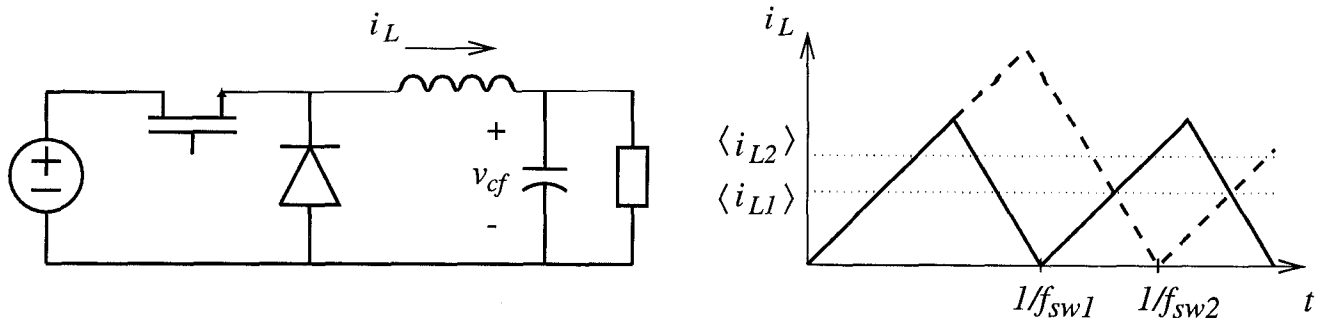
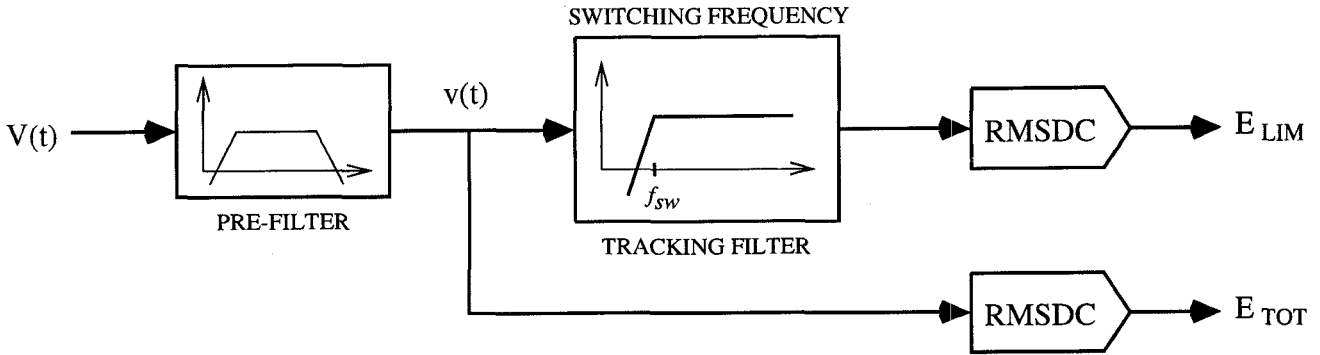


Figure 3 A buck converter cell operating at the edge of discontinuous conduction. The switching frequency is inversely proportional to the average output current.



**Figure 4** Structure of the frequency estimator used in the prototype system.  $E_{lim}$  is the rms of the filtered ripple,  $E_{tot}$  is the rms of the total ripple. These signals are used by the current-sharing controller.

kHz switching frequency, while 10% load corresponds to a 10 kHz switching frequency. The cell output current switching ripple causes a very small (<2%) ripple in the output voltage at the same fundamental frequency. It is the frequency content of this output voltage ripple which carries information about the average cell output current.

### B. Frequency Estimation

To decode the current-sharing information contained in the output voltage ripple, each cell employs a frequency estimator which detects whether any other cell is operating at a lower switching frequency. The estimator structure used in the prototype system, shown in Fig. 4, is composed of three stages: (1) a prefilter stage, (2) a frequency-tracking filter stage, and (3) an rms-to-dc conversion stage. The prefilter stage removes the low-frequency and high-frequency (noise) components of the output voltage, while amplifying the switching ripple component. The frequency-tracking filter is a high-pass filter whose cutoff frequency is continuously adjusted to fall just below the local cell switching frequency, in order to attenuate switching ripple components at frequencies below that of the local cell. The rms-to-dc conversion stage measures the rms of the switching ripple signals before and after the tracking filter. If the rms of the filtered switching ripple is lower than that of the unfiltered ripple, it indicates that one or more cells are operating at switching frequencies below that of the local cell. Thus, the estimator structure of Fig. 4 provides enough information to implement the current-sharing approach described previously.

The prefilter stage is a cascade of a second-order Butterworth high-pass filter ( $f_c = 500$  Hz), a second-order Butterworth low-pass filter ( $f_c = 40$  kHz), and a high-gain frequency-dependent amplifier. The frequency-dependent amplifier compensates for the fact that the magnitude of the voltage ripple across the capacitive output filter decreases with increasing frequency. For frequencies below 20 kHz, it acts as a differentiator to amplify ripple components by an amount proportional to their frequency. Above 20 kHz, it acts as an integrator to attenuate high frequency noise. The output of the prefilter stage is thus an amplified and frequency-compensated version of the output switching ripple, with high-order switching harmonics (and high-frequency noise) attenuated.

The frequency-tracking filter stage is a fourth-order Butterworth high-pass filter whose cutoff frequency is

continuously adjusted to 0.8 times the local switching frequency. A Butterworth filter is selected because it exhibits no peaking in its response near the cutoff frequency. The tracking filter is implemented using an LMF100 switched-capacitor filter whose clock frequency is derived from the local switching frequency.

To achieve the desired tracking filter cutoff frequency, the LMF100 clock frequency must be 80 times the local switching frequency. A frequency multiplier based on the 74VHC4046 phase-locked loop (PLL) IC is used to generate the LMF100 clock from the local gate drive waveform. A divide-by-eighty counter in the feedback path of the PLL yields a switched-capacitor filter clock frequency of 80 times the (input) switching frequency. This results in a tracking filter cutoff frequency of 0.8 times the switching frequency.

The rms-to-dc conversion stage of the frequency estimator measures the rms of the switching ripple signals before and after the tracking filter. It is implemented using AD637 integrated circuit rms-to-dc converters connected in the two-pole Sallen-Key filter arrangement. The averaging and filter capacitor values ( $C_{AV} = 0.022$   $\mu$ F,  $C_2 = C_3 = 0.047$   $\mu$ F) are selected to yield a 1% settling time of 8 ms. This is considered fast enough to track the variations in switching ripple frequency content while still suppressing ripple in the rms-to-dc converter outputs. The two rms-to-dc converter outputs form the output of the frequency estimator stage. Any difference between these signals indicates that another cell is operating at a lower switching frequency. This information is used by the current-sharing controller to achieve load balance with the other cells.

### C. Control Design

This section describes the design of the control circuitry used in the prototype converter system. A block diagram of the cell control structure used in the prototype system is shown in Fig. 5. In simplest terms, each cell can be viewed as having an inner current control loop, a middle voltage control loop, and an outer load-sharing control loop. The inner current loop, which maintains cell operation at the edge of discontinuous conduction, causes the average output current  $i_{out}$  to accurately track a current reference  $i_{ref}$ , and allows the cell power stage to be modeled as a controlled current source of value  $i_{ref}$  (yielding  $H(s) \sim 1$  in Fig. 5). It also inherently enforces a relationship between the cell switching frequency and average output current, thus encoding current sharing information on the output

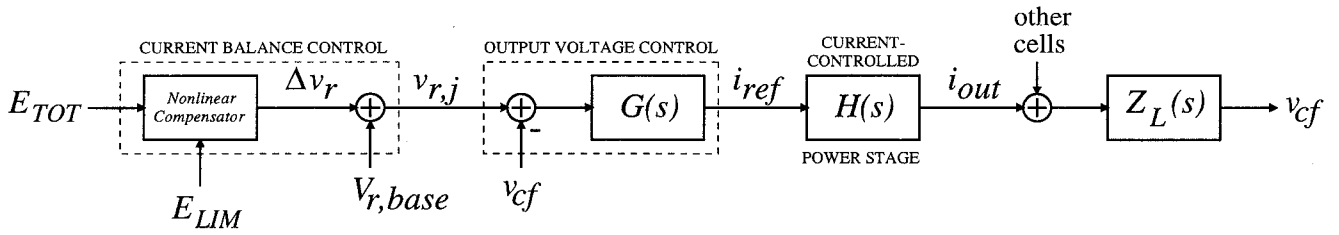


**Figure 5** Block diagram of the cell control structure used in the prototype system.

switching ripple.

To regulate the output voltage, each cell has a middle voltage control loop which generates the current reference for its inner loop based on the difference between a local voltage reference and the output voltage. The prototype system employs a lag compensator ( $\tau_p = 0.0159$ ,  $\tau_z = 0.00159$ , dc gain = 50 mA/V) for this purpose. This yields a voltage control bandwidth on the order of 100 Hz, with less than 5% load regulation over the load range of the cell. The output of the voltage control circuit has a clamp such that the commanded reference current is always within the specified load range of 1 - 10 mA.

To achieve load balance among cells, each cell has a slow outer current-sharing loop which operates by adjusting the local reference voltage  $v_{r,ref}$  over a limited range about a base value  $v_{r,base}$ . The individual converter references are shifted via integral control based on the difference between the two frequency estimator outputs minus a small offset. That is, the system uses the difference between the rms of the total switching ripple and the rms of the switching ripple components at frequencies of the local cell and higher, minus an additional offset; i.e.

$$\frac{dv_{r,j}}{dt} = K_j [E_{tot} - E_{lim} - \Delta E] \quad (2)$$

where  $K_j$  is the (integral) control gain,  $E_{tot}$  and  $E_{lim}$  are the two frequency estimator outputs, and  $\Delta E$  is the offset. The  $j^{th}$  reference is adjustable over a small range from a base value  $v_{r,j,base}$  to a maximum value  $v_{r,j,max}$  (which is about 5% larger than the base value), and is prevented from going outside this range. The offset  $\Delta E$  guarantees that the reference of the lowest switching frequency (highest current) cell will always be driven down towards its base value so that current sharing can be achieved.

To implement this outer-loop control structure, the prototype system uses the reference adjustment circuitry provided in the UC3907 load-sharing IC. The UC3907 is designed to implement a single-wire current-sharing scheme in which the local voltage reference is adjusted based on the difference between the highest cell current and the local cell current, minus a small offset [10]. By properly scaling and shifting the two outputs of the frequency estimator and using them in place of the local and highest current inputs of the UC3907, the UC3907 can instead be caused to adjust its local reference voltage as previously described. The integrating compensator implemented in the UC3907 yields a current-sharing control bandwidth on the order of a Hertz.

The three control loops operate together to properly regulate the output voltage of the system while maintaining current sharing among cells. While other design approaches are

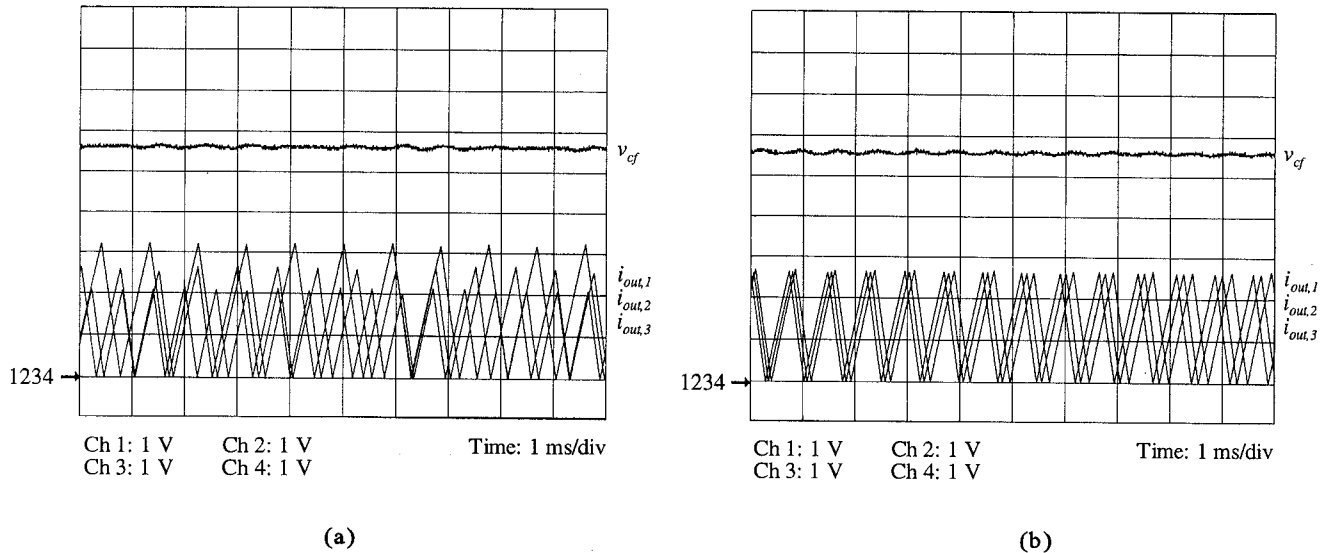


**Figure 6** Current-sharing characteristics of the prototype system at approximately 66% of full load ( $R_{load} \approx 278\Omega$ ). (a) Without current-sharing control. (b) With current-sharing control. Current signals are represented at a scale factor of 200 V/A.

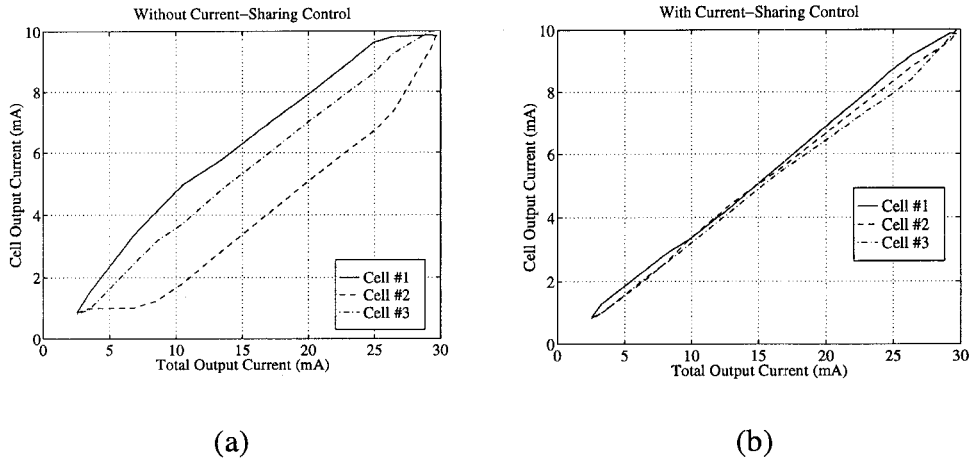


**Figure 7** The static current-sharing characteristic of the prototype system. (a) without current-sharing control. (b) with current-sharing control.

possible, this multilayered control strategy has been found to be both simple and effective.

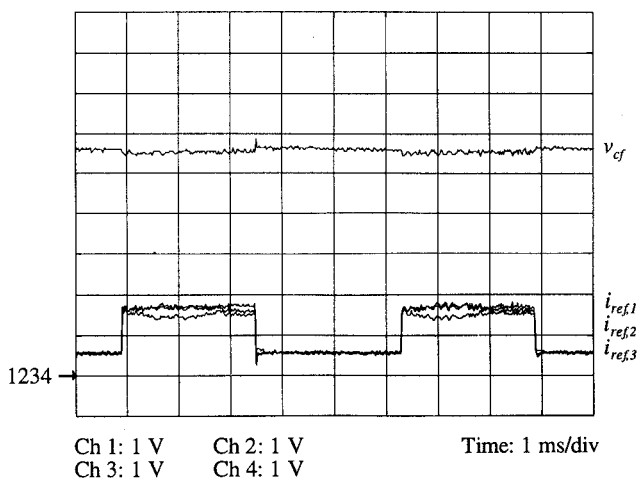
#### IV. EXPERIMENTAL EVALUATION

This section presents an evaluation of the switching ripple method of current-sharing control using a 3-cell prototype system of the design presented in the previous section. Additional results can be found in [16]. It should be noted that the approach is independent of the number of cells in the system, and can be applied to systems with an arbitrary number of cells. Figure 6 shows operation of the prototype system at approximately 66% of full load both with and without current-sharing control. Without current-sharing control, there is a significant imbalance in average output current among the three cells. The inverse relationship between switching frequency and average output current is also apparent. With current-sharing control, the switching frequencies and average cell

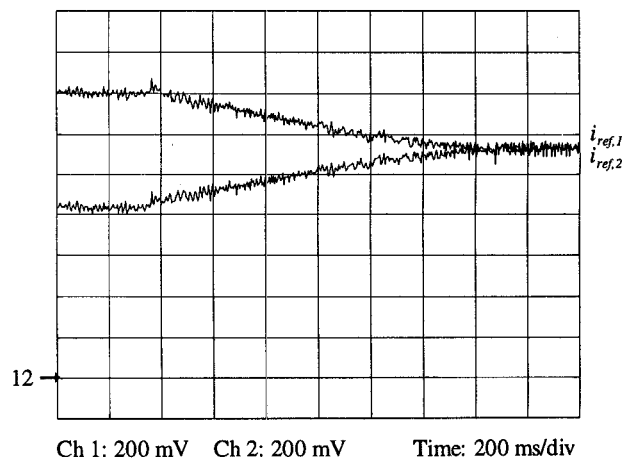
output currents are almost precisely equal. This high degree of current sharing is achieved by using the information encoded in the frequency content of the output switching ripple, without additional interconnections.

Figure 7 shows the static current-sharing characteristic over the load range of the system both with and without current-sharing control. Without current sharing, there are significant current imbalances over much of the load range, while with current sharing the cells share current to within 5% of the average over the entire load range. This high degree of active current sharing is obtained with less than 5% load regulation over the entire load range.

Current-sharing behavior was also investigated under transient conditions. Figure 8 shows the current-sharing behavior for load steps between 673  $\Omega$  and 224  $\Omega$ , corresponding to approximately 27% and 83% of full load. The current-sharing behavior is seen to be stable for even large load steps. Figure 9 shows the reference current transient response



**Figure 8** Transient response for load steps between 224  $\Omega$  and 673  $\Omega$  (approximately 27% and 83% of full load). Currents are represented at 200 V/A.



**Figure 9** Current reference transient response for two cells when current sharing is turned on with  $R_L = 500 \Omega$ . Currents are represented at 200 V/A.

for two cells when current-sharing control is turned on. Again, accurate current sharing is rapidly achieved with stable dynamics. What may be concluded from these results is that the switching ripple method can be used to achieve accurate static and dynamic current sharing without the need for additional interconnections among cells.

## V. CONCLUSIONS

This paper presents the implementation and experimental evaluation of a new current-sharing approach for paralleled power converters. This approach, which is based on encoding the current-sharing information in the switching ripple of the converter cells, eliminates the need for additional current-sharing interconnections among converters. Practical implementation of the approach is addressed, including methods for controlling the cell switching patterns, decoding the current-sharing information from the output switching ripple, and controlling the output voltage and current sharing. An experimental evaluation of the new current-sharing approach based on a 3-cell prototype system is also presented. It is shown that accurate and stable current sharing is obtainable over a wide load range using this approach.

## ACKNOWLEDGMENTS

The authors would like to gratefully acknowledge the support for this research provided by the Bose Foundation and the Office of Naval Research. Kenji Sato thanks the Central Japan Railway Company for supporting him during this research.

## REFERENCES

- [1] J.G. Kassakian, "High Frequency Switching and Distributed Conversion in Power Electronic Systems," *Sixth Conference on Power Electronics and Motion Control (PEMC 90)*, Budapest, 1990.
- [2] J.G. Kassakian and D.J. Perreault, "An Assessment of Cellular Architectures for Large Converter Systems," *First International Conference on Power Electronics and Motion Control*, Beijing, 1994, pp. 70-79.
- [3] K.T. Small, "Single Wire Current Share Paralleling of Power Supplies," *U.S. Patent 4,717,833*, 1988.
- [4] R. Wu, T. Kohama, Y. Kadera, T. Ninomiya, and F. Ihara, "Load-Current-Sharing Control for Parallel Operation of DC-to-DC Converters," *IEEE Power Electronics Specialists Conference*, 1993, pp. 101-107.
- [5] T. Kohama, T. Ninomiya, M. Shoyama, and F. Ihara, "Dynamic Analysis of Parallel Module Converter System with Current Balance Controllers," *1994 IEEE Telecommunications Energy Conference Record*, 1994, pp. 190-195.
- [6] T. Kohama, T. Ninomiya, M. Wakamatsu, and M. Shoyama, "Static and Dynamic Response of a Parallel-Module High Power-Factor Converter System with Current-Balancing Controllers," *IEEE Power Electronics Specialists Conference*, 1996, pp. 1198-1203.
- [7] M. Jovanovic, D. Crow, and L. Fang-Yi, "A Novel, Low-Cost Implementation of 'Democratic' Load-Current Sharing of Paralleled Converter Modules," *IEEE Trans. Power Electron.*, Vol. 11, No. 4, July 1996, pp. 604-611.
- [8] V.J. Thottuvelil and G.C. Verghese, "Stability Analysis of Paralleled DC/DC Converters with Active Current Sharing," *IEEE Power Electronics Specialists Conference*, 1996, (in press).
- [9] D. Maliniak, "Dense DC-DC Converters Actively Share Stress," *Electronic Design*, Jan. 21, 1993, pp. 39-44.
- [10] M. Jordan, "UC3907 Load Share IC Simplifies Parallel Power Supply Design," *Unitrode Application Note U-129*, Unitrode Corp., Merrimack, NH.
- [11] J. Bocek and C. Liu, "Determining Current Sharing Criterion for Parallel Operation of Power Converters in Multi-Module Bus Systems," *IEEE Power Electronics Specialists Conference*, 1990, pp. 870-879.
- [12] J. Glaser and A. Witulski, "Output Plane Analysis of Load-Sharing in Multiple-Module Converter Systems," *IEEE Transactions on Power Electronics*, Vol. 9, No. 1, Jan. 1994, pp. 43-50.
- [13] J. Dixon and B. Ooi, "Series and Parallel Operation of Hysteresis Current-Controlled PWM Rectifiers," *IEEE Transactions on Industry Applications*, Vol. 25, No. 4, July/August 1989, pp. 644-651.
- [14] D.J. Perreault, R. Selders, and J.G. Kassakian, "Frequency-Based Current-Sharing Techniques for Paralleled Power Converters", *1996 IEEE Power Electronics Specialists Conference*, Baveno, Italy, pp. 1073-1079.
- [15] D.J. Perreault, R.L. Selders, and J.G. Kassakian, "Implementation and Evaluation of a Frequency-Based Current-Sharing Technique for Cellular Converter Systems," *IEEE Africon '96*, Matieland, South Africa, pp. 682-686.
- [16] K. Sato, "A Switching Ripple Based Current Sharing Control System for Cellular Converters," S.M. Thesis, *M.I.T. Department of Electrical Engineering and Computer Science*, June 1997.
- [17] D. Perreault, "Design and Evaluation of Cellular Power Converter Architectures," Ph.D. Thesis, *M.I.T. Department of Electrical Engineering and Computer Science*, June 1997.